ACS OMEGA

Open Access

http://pubs.acs.org/journal/acsodf

Article

Solvent-Free Synthesis of HKUST-1 with Abundant Defect Sites and Its Catalytic Performance in the Esterification Reaction of Oleic Acid

Ahmed S. Abou-Elyazed,* Abdelhalim I. Ftooh, Yinyong Sun,* Asmaa G. Ashry, Amira K. F. Shaban, Ahmed M. El-Nahas, and Ahmed M. Yousif

Cite This: *ACS Omega* 2024, 9, 37662−37671

Read Online

ACCESS | Metrics & More | Article Recommendations | Supporting Information

ABSTRACT: HKUST-1 has received increasing attention because of its potential applications in many fields, such as heterogeneous catalysis, sensors, gas storage, and separation. Herein, we report that HKUST-1 can be facilely prepared by heating a ground mixture of copper nitrate trihydrate and 1,3,5-benzenetricarboxylic acid in an autoclave at 80 °C for 10 h. The data from nitrogen sorption show that the obtained material, named HKUST-1-free, possesses a high BET specific surface area of 1671 m^2/g and a pore volume of 0.8 cm^3/g. The results from acid−base titration indicate that the number of defect sites in HKUST-1-free is more than that in HKUST-1-solvent prepared by the solvothermal method. As a heterogeneous catalyst, HKUST-1-free gave a high yield (91%) of methyl oleate in the esterification reaction of oleic acid with methanol at room temperature compared to HKUST-1-solvent (70%). Additionally, it is proven that HKUST-1-free is a heterogeneous catalyst and can be reused.

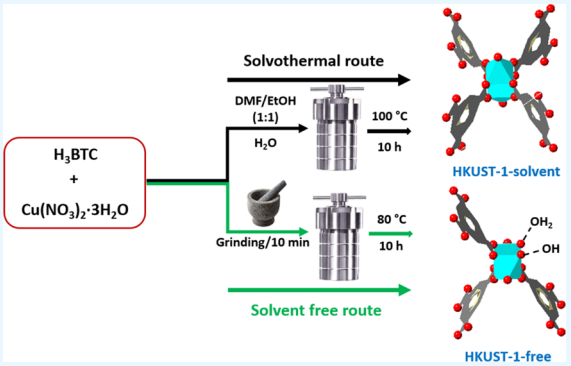

1. INTRODUCTION

In recent years, the world has become increasingly dependent on fossil fuels, making it imperative to seek out alternative, sustainable energy sources.[1] Renewable energy sources such as solar energy, wind energy, hydroelectric energy, and biofuel energy can enhance a country's energy security on a global scale.[2] As a result, the use of renewable fuels is a simple and cost-effective solution. In this regard, biofuels derived from biomass conversion are considered one of the most promising renewable energy sources because of the advantages involving the lack of toxic oxides that contribute to global warming and air pollution and their easy biodegradability.[3]

As a type of liquid biofuel, biodiesel is industrially produced in the presence of homogeneous alkaline/or acid catalysts, since they are highly efficient at relatively low temperatures.[4] However, the difficulties in the catalyst recovery with the undesirable wastewater obtained in the downstream purification processes are the major constraints to the homogeneous catalyzed process.[5] To solve these problems, the recyclable and readily separable heterogeneous catalysts to produce biodiesel have been widely investigated.[5,6] Examples of heterogeneous catalysts that were utilized in biodiesel production include sulfonated mesoporous carbon (SMC),[7] acidic ionic exchange resin,[8] CaO/ZrO_2, CaO/MoO_3/SBA-15,[9] Mg−Al hydrotalcites,[10] and heteropoly acids,[11] which were shown to have high catalytic activities in the transesterification reactions. However, the above-mentioned materials suffer from demerits such as low surface area and lacking tunability and porosity.

In recent decades, metal−organic frameworks (MOFs) have been one of the rapidly growing research fields due to their varied pore structures, high surface areas, and easy functionalities.[12] As an important member of MOFs, HKUST-1 is widely studied owing to its potential as a heterogeneous catalyst, an adsorbent, a sensor, and so on.[13] Up to now, several strategies for the synthesis of HKUST-1 have been reported including microwave-assisted synthesis,[14] ultrasonic synthesis,[15] mechanochemical synthesis,[16−19] and conventional hydro/solvothermal synthesis.[20−23] Commonly, the methods mentioned above would involve the use of solvent or cumbersome procedures.

In this work, we report that HKUST-1 with a high surface area and pore volume could be prepared by the direct interaction of 1,3,5-benzenetricarboxylic acid with copper nitrate trihydrate under solvent-free conditions. The obtained materials were characterized by various techniques, including XRD, N_2 sorption, FT-IR, SEM, and NH_3-TPD. Additionally, their catalytic performance was evaluated by the esterification reaction of oleic acid with methanol. The effect of some

Received: February 26, 2024
Revised: August 1, 2024
Accepted: August 16, 2024
Published: August 24, 2024

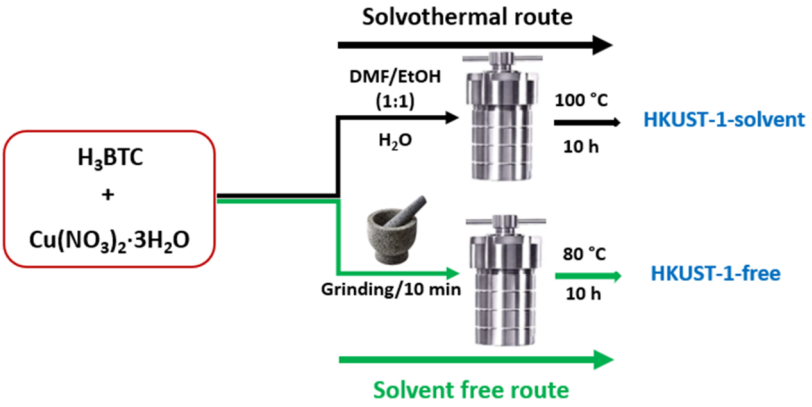

Figure 1. Schematic representation of various synthetic routes of HKUST-1.

reaction conditions such as catalyst loading, the molar ratio of methanol to oleic acid, reaction temperature, and time on catalytic performance was examined. Furthermore, the reusability of such a catalyst was also investigated.

2. EXPERIMENTAL SECTION

2.1. Materials. All chemicals were used directly as received: 1,3,5-benzenetricarboxylic acid (H_3BTC), copper nitrate trihydrate $Cu(NO_3)_2{\cdot}3H_2O$, copper chloride ($CuCl_2$), copper acetate hydrate, oleic acid (Tianjin Zhi Yuan, 98%), methanol (Sinopharm, 99.7%), *N*,*N*-dimethylformamide (DMF, Sinopharm, 99%), ethanol (Sinopharm, 99%), phenolphthalein, potassium bromide, sodium hydroxide, hydrochloric acid (Sinopharm, 37%), and potassium hydroxide (Sinopharm, 99.5%).

2.2. Synthesis of Materials. The facile synthesis of HKUST-1 was carried out mainly based on our previous works.[24,25] Typically, $Cu(NO_3)_2{\cdot}3H_2O$ (519 mg) as the metal precursor and H_3BTC (250 mg) were pulverized together for about 10 min at room temperature. Then, the obtained materials were transferred into a Teflon line autoclave at different crystallization times and temperatures. After cooling to room temperature, the resultant blue powder was treated with ethanol at 70 °C for 2 h and then dried for 12 h at 150 °C under vacuum. The final samples are denoted HKUST-x-t, where x is the crystallization temperature (°C) and t is the crystallization time (h) (see Figure S1).

Comparatively, conventional HKUST-1 was prepared according to the literature.[22] H_3BTC (250 mg) was dissolved in 30 mL of a 1:1 mixture of ethanol/DMF. In another flask, $Cu(NO_3)_2{\cdot}3H_2O$ (519 mg) was dissolved in 15 mL of water. The two solutions were mixed and stirred for 10 min. Then, the mixture was transferred into a Teflon line autoclave and heated at 373 K for 10 h. After cooling to room temperature, the obtained blue powder was treated with ethanol at 70 °C for 2 h and then dried at 150 °C for 12 h under vacuum. The final sample was denoted HKUST-1-solvent. A scheme of various synthetic routes of HKUST-1 is shown in Figure 1.

2.3. Scalable Synthesis of HKUST-1-free. 40 mmol of $Cu(NO_3)_2{\cdot}3H_2O$ and 22.22 mmol of BTC were combined and manually ground in a mortar for approximately 10 min at room temperature. The resultant mixture was then transferred to a 50 mL autoclave and subjected to crystallization at 80 °C for 10 h. Following the crystallization process, the mixture was allowed to cool to room temperature. The blue solid formed was subsequently treated with ethanol at 70 °C for 2 h. Finally, the washed solid was dried under vacuum at 150 °C for 12 h.

2.4. Characterization. The catalysts were characterized by XRD, SEM, FT-IR, BET, XPS, and TGA. Powder X-ray diffraction (PXRD) analysis was performed on a Rigaku D/Max-2550 diffractometer furnished with a SolX Detector-Cu K radiation with λ = 1.542 Å. Data were enrolled by step scanning at $2\theta = 0.02°$ per second from 5 to 50°. The morphology of the catalyst was studied using a SUPRA 55 scanning electron microscope (SEM) with an acceleration voltage of 20 kV. Nitrogen sorption experiments were performed at −196 °C on a 3H-2000PS1 Gas Sorption and Porosimetry system. The samples were regularly arranged for examination after degassing at 150 °C for 2 h under vacuum until the final pressure reached 1×10^{-3} Torr. Fourier transform infrared (FT-IR) spectroscopy was performed on a NicoLET iS10 spectrometer. Spectra were recorded with the KBr pellet technique using a Bruker Equinox 55 Fourier transform infrared spectrophotometer, and diffuse reflectance spectra were scanned in the range of 500−4000 cm^{-1} with a resolution (2 cm^{-1}) of 100 scans for each measurement. Thermogravimetric analysis (TGA) was conducted on a Shimadzu TA-50. Potentiometric acid−base titrations were completed with a Metrohm Titrando 905 autotitrator equipped with Dosino 800 dosing units. X-ray photoelectronic spectroscopy (XPS) was carried out using monochromatic X-ray Al K-Alpha radiation on the US Thermo Scientific K--alpha apparatus.

2.5. Catalytic Test. Esterification reactions were carried out in a 50 mL two-necked glass flask equipped with a condenser. Typically, the reactions were performed with oleic acid (1 mL) and methanol (8 mL) using a 4% catalyst (based on the fatty acid weight) at 25 °C for 1 h. After the reaction, the catalyst was collected by centrifugation, and the excess of methanol and water were removed by distillation at 100 °C for 1 h. The yield of methyl oleate was estimated by a titration method (0.1 M alcoholic KOH as a titrant) in the presence of phenolphthalein as an indicator. The amount of KOH consumed was enlisted. The conversion of oleic acid (OA) was assessed using eq 1. Methyl oleate was also quantitatively analyzed by gas chromatography on an Agilent 7890A with an FID detector using a 30 m packed HP5 column. All experiments were carried out in duplicate or triplicate, and the results are consistent with a standard deviation of ±0.02 mass %.

$$\text{conversion} = \frac{a_i - a_f}{a_i} \times 100\% \quad (1)$$

https://doi.org/10.1021/acsomega.4c01852
ACS Omega 2024, 9, 37662−37671

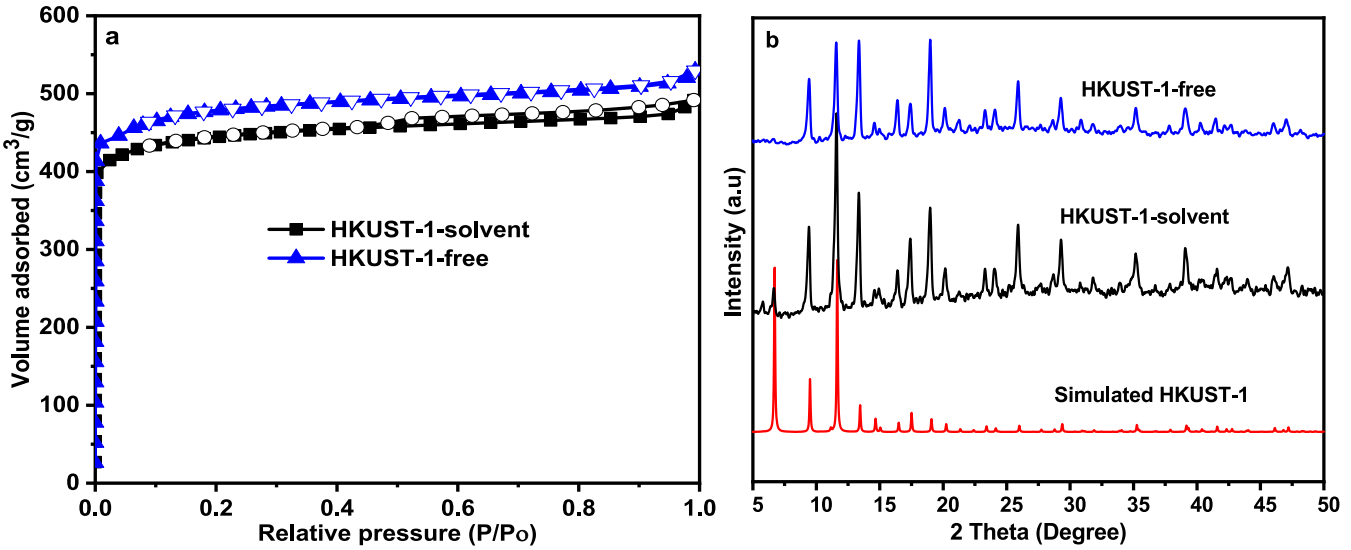

Figure 2. Nitrogen sorption isotherms (b) and XRD patterns (b) of HKUST-1-solvent and HKUST-1-free.

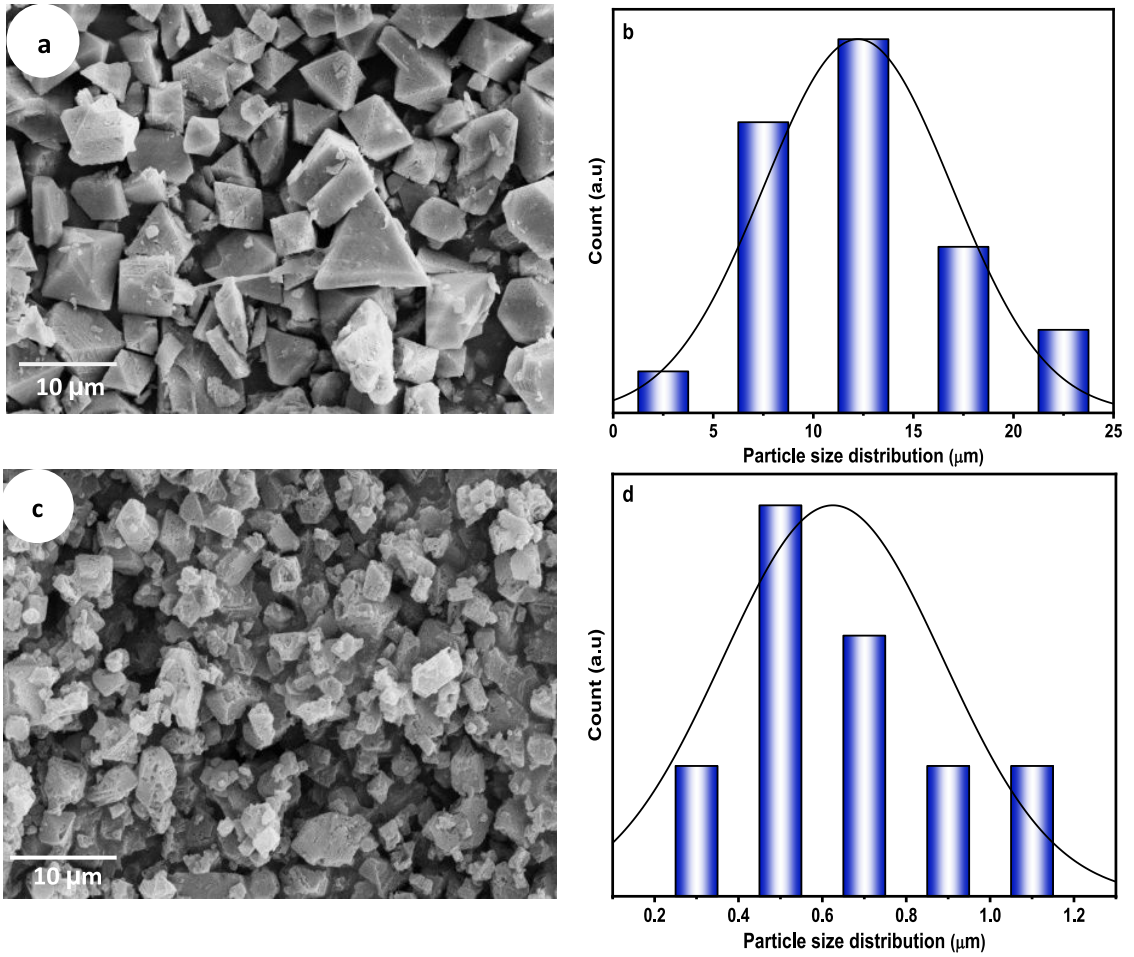

Figure 3. SEM images and particle size distribution of HKUST-1-solvent (a, b) and HKUST-1-free (c, d).

Where, a_i *and* a_f are the initial and final concentrations of OA, respectively.

3. RESULTS AND DISCUSSION

3.1. Characterization. The optimization of the synthetic parameters under solvent-free conditions was investigated. The nitrogen sorption isotherms of the obtained materials are displayed in Figure S1, and corresponding sorption data are shown in Table S1. As seen, all of the samples show type I sorption isotherms, indicating the presence of micropores. Differently, the sample prepared at 80 °C for 10 h possesses the highest surface area (1671 m^2/g) and pore volume (0.8 cm^3/g;

https://doi.org/10.1021/acsomega.4c01852
ACS Omega 2024, 9, 37662−37671

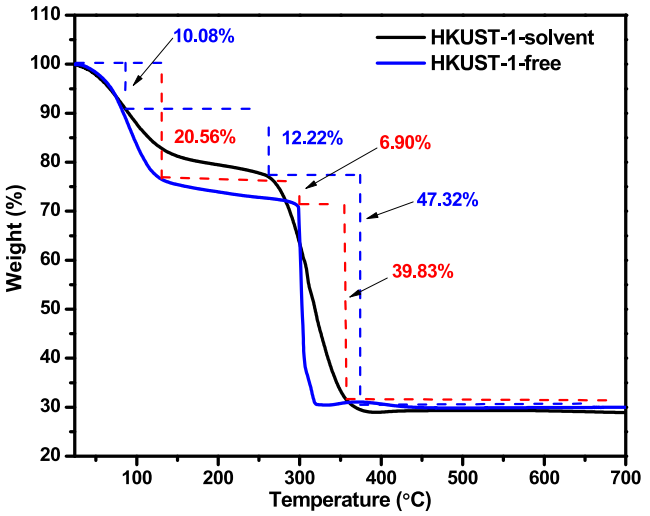

Figure 4. TGA curves of HKUST-1-solvent and HKUST-1-free.

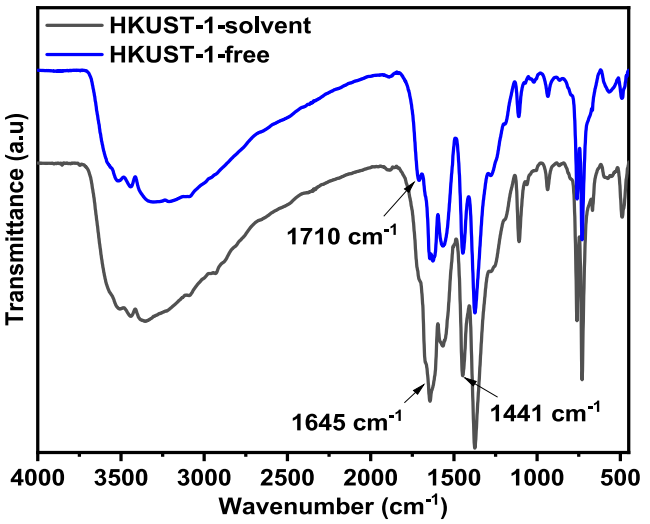

Figure 6. FT-IR spectra of HKUST-1-solvent and HKUST-1-free.

Figure 2a) among these synthesized materials. Considering that high surface area could be beneficial for improving catalytic efficiency, this material named HKUST-1-free is selected for the following studies.

For comparison, a sample named HKUST-1-solvent was prepared under solvothermal conditions. Figure 2b shows the XRD patterns of HKUST-1-solvent and HKUST-1-free. It can be seen that both samples exhibited well-resolved diffraction patterns, which are in good agreement with the simulated XRD patterns for HKUST-1.[26,28] This result indicates that HKUST-1 has been successfully synthesized by both methods. Differently, HKUST-1-free possesses a higher BET surface area and pore volume than HKUST-1-solvent (1352 m^2/g and 0.7 cm^3/g, respectively). Additionally, the effect of the copper source on the solvent-free synthesis of HKUST-1 was also studied. As shown in Figure S2, all of the samples displayed XRD patterns belonging to the HKUST-1 structure, indicating that the copper source had no big influence on the formation of HKUST-1.

Figure 3 displays the SEM images and particle size distribution of HKUST-1-solvent and HKUST-1-free. HKUST-1-solvent exhibited a morphology of a cuboctahedra shape with a particle size from 2 to 10 μm (Figure 4a). Comparatively, HKUST-1-free showed a morphology of a cuboctahedra shape with a particle size from 0.5 to 2 μm (Figure 3b). Obviously, HKUST-1-free possessed a smaller particle size than HKUST-1-solvent, which can be the main reason why HKUST-1-free possesses a higher BET surface area than HKUST-1-solvent. Moreover, the simulated SEM images for both samples showed a difference in surface roughness, indicating that the preparation method would influence not only particle size but also the surface morphology of samples (Figure S3).

Based on our earlier work, it is known that the solvent-free method easily creates defects in the structure of MOFs. To acquire the information on defect sites in HKUST-1, TGA curves were measured. As shown in Figure 4, both samples show three distinct weight loss. The first weight loss below 130 °C can be assigned to the removal of the surface water molecules. The second one in the range of 130−255 °C could be attributed to the removal of the water molecules present in the channels and coordinated to the metal centers in the structure. The third loss above 255 °C corresponded to decomposition of the organic linkers. It was noted that a weight loss of 39.8% for HKUST-1-free was lower than that of 47.3% for HKUST-1-solvent,

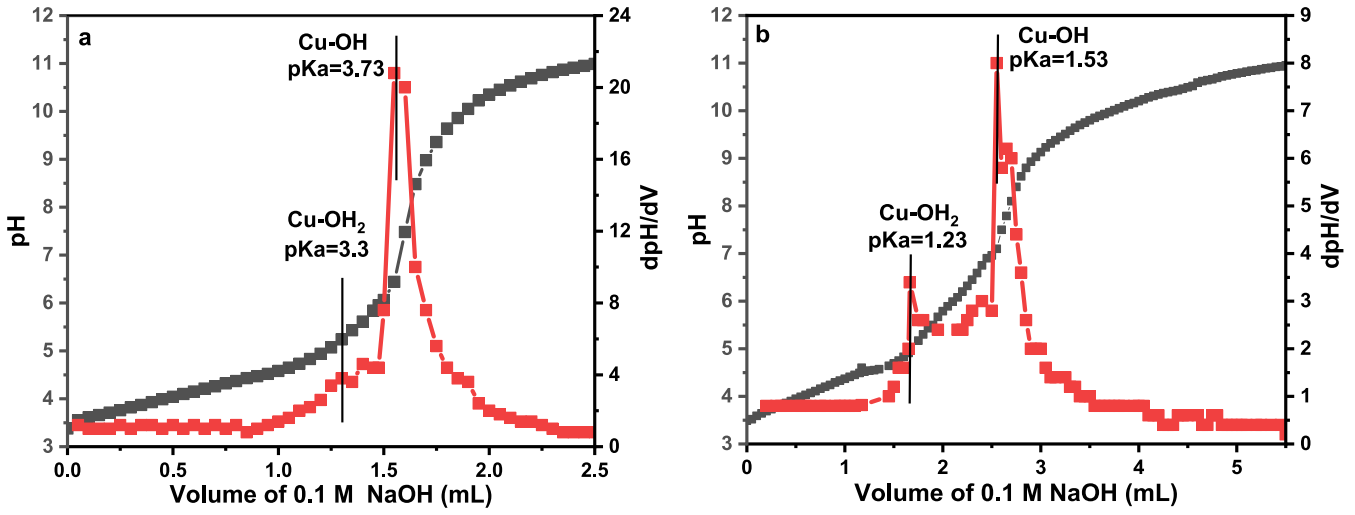

Figure 5. Acid−base titration curves (black) and first-derivative curve (red) of HKUST-solvent (a) and HKUST-1-free (b).

https://doi.org/10.1021/acsomega.4c01852
ACS Omega 2024, 9, 37662−37671

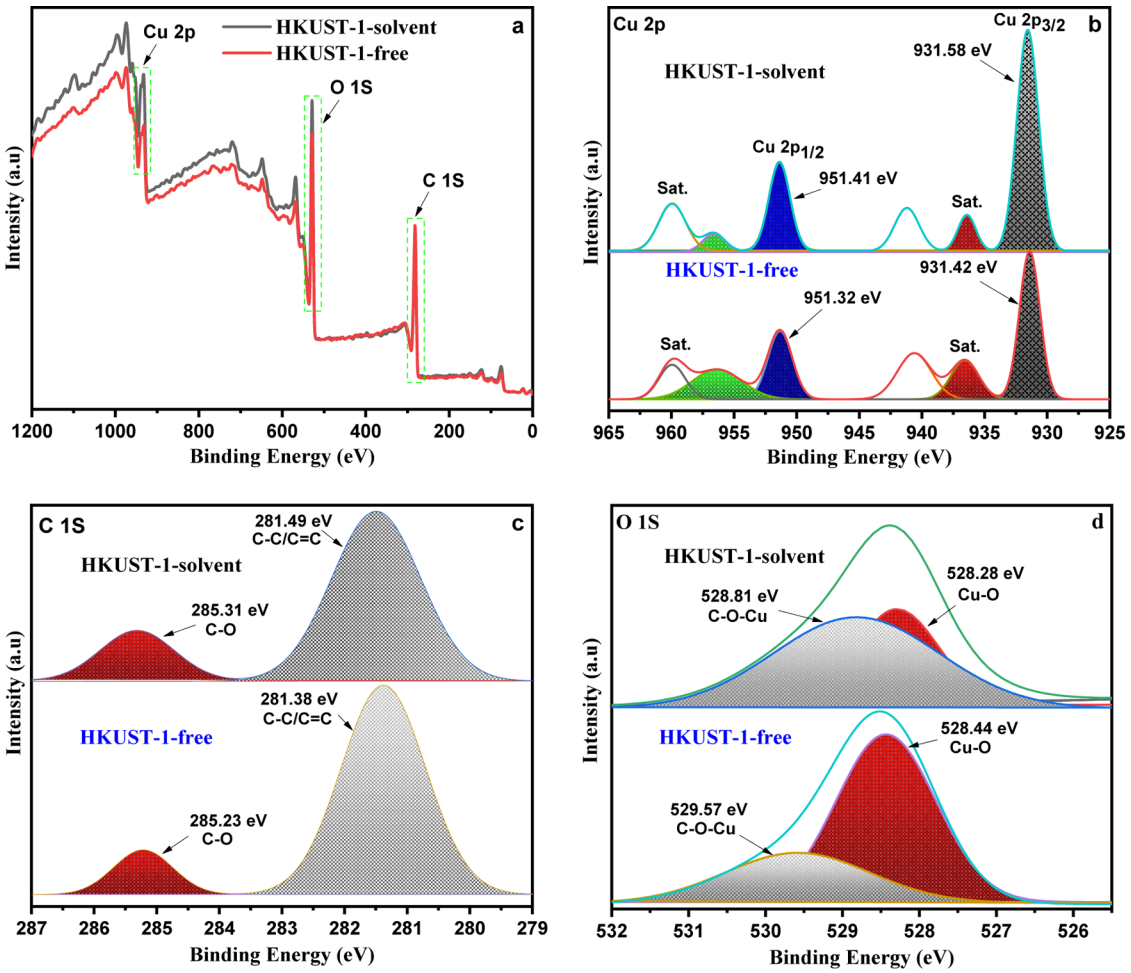

Figure 7. XPS results of HKUST-1-solvent and HKUST-1-free: (a) XPS survey spectra, (b) Cu 2p spectra, (c) O 1s spectra, and (d) C 1s spectra.

suggesting that the missing linkers in HKUST-1-free should be higher than that in HKUST-1-solvent. That means that more defect sites should be formed in HKUST-1-free.

To demonstrate this point, potentiometric acid−base titration is used to determine the number of defect sites.[27] Generally, each SBU should be connected to 2 BTC linkers if there are no defects in the structure of HKUST-1. When the defects are created, two types of protons ($Cu-OH_2$ and Cu−OH) that cap the defect sites are available for titration. The titration curves for HKUST-1-solvent and HKUST-1-free are shown in Figure 5. To better visualize the various equivalence points, the first derivative of the titration curve is also plotted. The results exhibit two distinct equivalence points corresponding to pK_a values of 3.3 and 3.73 for HKUST-1-solvent. In comparison, the pK_a values are 1.23 and 1.53 for HKUST-1-free. Based on the quantification calculations (Tables S3 and S5), HKUST-1-solvent gave a missing linker number of 0.324 in the structure. Comparatively, the number of missing linkers in HKUST-1-free reached 0.517. The number of defect sites in HKUST-1-free is more than that in the HKUST-1-solvent. As is known, a solvent-free method may lead to the creation of defects in MOFs. One common type of defect in MOFs prepared by solvent-free methods is the presence of missing or incomplete linker units. This can occur due to uneven distribution of reactants or incomplete coordination between metal ions and ligands. Another type is the formation of a nonuniform crystal structure or crystallographic disorder, as presented in Figure 3a,c, which could be attributed to the variations in reaction conditions or incomplete crystallization.[28−31]

The FT-IR spectra of HKUST-1-solvent and HKUST-1-free are shown in Figure 6. The typical vibration frequencies at 1645 and 1441 cm^{-1} are assigned to the asymmetric and symmetric vibrations of the carboxylates, respectively. An absorption band characteristic of C═O stretching from free carboxylic acids (uncoordinated) could be observed at around 1710 cm^{-1} for HKUST-1-free, whereas this band is absent in HKUST-1-solvent. The results suggest that the defects should be formed in the structure of HKUST-1-free. Additionally, the presence of −COOH groups in HKUST-1-free is further confirmed by the absorption bands at around 1107 cm^{-1} (C−O stretching) and 1266 cm^{-1} (−OH bending), which are typical bands of carboxylic acids.

X-ray photoelectron spectroscopy is a valuable technique to determine the oxidation states of elements and the chemical composition of materials. Figure 7a displays the complete survey spectra of HKUST-1-solvent and HKUST-1-free. As seen, the elements of Cu, O, and C are present in both samples. The results about the binding energies of Cu 2p from Figure 7b suggest that copper in HKUST-1 is predominantly Cu^{2+}.[32] Furthermore, the binding energies of around 936.43 and 956.65 eV in both samples confirm the presence of Cu^{+}. It is noted that the intensity of these peaks in HKUST-1-free is higher than that in HKUST-1-solvent, indicating that the content of Cu^{+} in HKUST-1-free might be relatively abundant. Figure 7c,d

https://doi.org/10.1021/acsomega.4c01852
ACS Omega 2024, 9, 37662−37671

Table 1. Comparison of the Catalytic Performance with Some Representative MOF Catalysts Used in the Esterification of OA

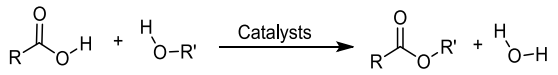

	reaction conditions					
Catalysts	Temp. (°C)	Time (h)	Volume ratio of MeOH and OA	Catalyst loading (%)	Yield (%)	Refs
blank	25	1	8:1	4	37	this work
HKUST-1-solvent	25	1	8:1	4	78	this work
HKUST-1-free	25	1	8:1	4	91	this work
Ni-MOF	160	5	2.6:1	3	55	34
UiO-66(Zr)-green	60	4	5:1	6	86	35
UiO-66(Zr)-solvent	60	4	5:1	6	43	35
HPW@MIL-100	111	5	7.5:1	15	40	36
MIL-125(Ti)	130	8	9:1	9	68	36
MOF-808(Zr)	130	8	9:1	9	88	37
UiO-66(Zr/Ca)	60	4	5:1	6	98	35
UiO-66(Zr/Sn)	60	4	5:1	6	99	38

presents the high-resolution XPS results of C 1s. The peaks at binding energies of 281.4 and 285.3 eV can be assigned to C−C/C═C and C−O bonds, respectively. Deconvolution of the O 1s spectrum in HKUST-1 samples reveals the presence of two types of bonds (Figure 7d). The peaks at approximately 528.28 and 528.81 eV for HKUST-1-solvent and at 528.44 and 529.57 eV for HKUST-1-free are ascribed to the O−Cu and C−O−Cu bonds, respectively.[33] The peak shift from the C−O−Cu bond toward higher binding energy in HKUST-1-free confirms a change in the environment around the Cu clusters, possibly resulting from the missing linker, suggesting that the amount of Cu^{+} in HKUST-1-free is higher than in HKUST-1-solvent.

3.2. Comparison of the Catalytic Activity of Various Catalysts. A comparison of the catalytic performances of various catalysts was made. As shown in Table 1, the conversion of OA is only 37% if no catalyst is used. Comparatively, when HKUST-1-free and HKUST-1-solvent are used as catalysts, the conversions of OA reached 91 and 78%, respectively. As seen, HKUST-1-free showed higher catalytic activity than HKUST-1-solvent, which could be related to the presence of more acid sites in HKUST-1-free, as demonstrated by acid−base titrations. In addition, the catalytic activity of HKUST-1-free has also been compared with some reported MOF catalysts used in the esterification of OA.[33−35] Among them, it can be seen that the catalytic performance of HKUST-1-free is still outstanding, although the reaction conditions are different in some cases. Based on the structure of HKUST-1, a catalytic reaction mechanism over HKUST-1-free is proposed in Scheme 1, which is consistent with the classic catalytic mechanism over Lewis and Bronsted acids. Herein, unsaturated Cu^{2+} centers acted as Lewis acids for the coordination with the carbonyl group of oleic acid to form a tetrahedral intermediate (carbocation) first. Then, Bronsted acid activates methanol to combine with carbocation, which is dehydrated to form methyl oleate and water. Finally, the catalyst was recovered for the next cycle of the catalytic reaction.

3.3. Effect of Reaction Conditions on the Catalytic Performance of HKUST-1-free. The impact of the OA/methanol volume ratio on the catalytic performance of HKUST-1-free was investigated (Figure 8a). Notably, the yield of methyl oleate was enhanced from 79 to 91% by increasing the OA/methanol volume ratio from 1:4 to 1:12. Obviously, a large volume ratio of OA/methanol helps improve catalytic activity. As reported, OA could be easily adsorbed on the surface of the catalyst to give a tetrahedral intermediate (carbocation). Thus, a greater volume ratio of OA/methanol would move the reaction ahead and supply a methanol nucleophilic attack on the intermediate, resulting in methyl oleate. Considering that the enhanced extent of the catalytic performance is restricted by the continuous rise of the OA/methanol volume ratio, an OA/methanol volume ratio of 1:8 was selected for the following studies (Figure 8a).[1,5,39]

Subsequently, the impact of catalyst loading was investigated. The yield of methyl oleate increases dramatically with the quantity of catalyst loading from 2 to 4 wt %, reaching a maximum yield of 90% at 4 wt % (Figure 8b). This improved yield might be due to a greater number of accessible acid sites in the reaction system. However, the yield of methyl oleate would decrease due to the rise in viscosity in the reaction system when the quantity of catalyst loading was further increased.[40,41] The influence of reaction time was assessed using a catalyst dosage of 4 wt %. Figure 8c shows that the reaction yields a high value of 84% at 60 min. Furthermore, increasing the reaction time marginally increased the yield of methyl oleate.[42] In addition, the effect of reaction temperature was investigated under the following conditions: a catalyst loading of 4 wt %, a reaction time

Scheme 1. Proposed Reaction Mechanism over HKUST-1 in the Esterification of OA with Methanol

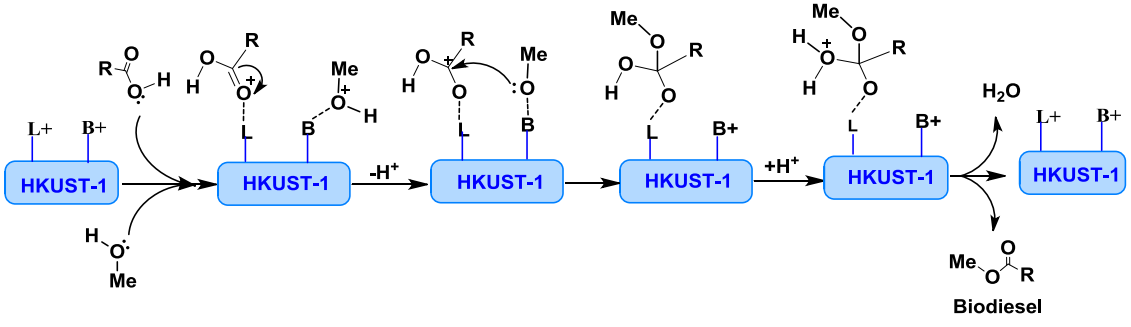

https://doi.org/10.1021/acsomega.4c01852
ACS Omega 2024, 9, 37662−37671

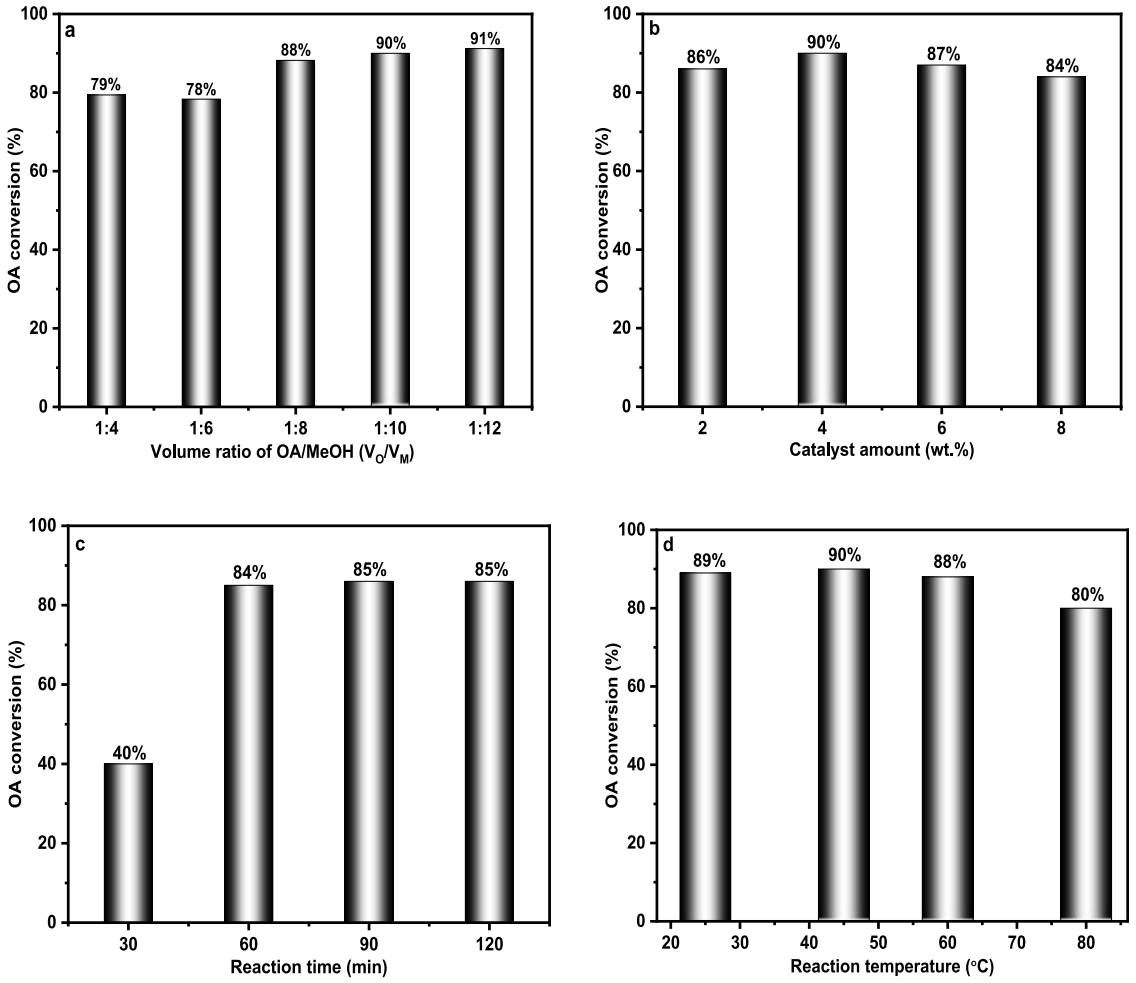

Figure 8. Influence of reaction conditions on the catalytic performance of HKUST-1-free: (a) OA/MeOH volume ratio, (b) catalyst amount, (c) reaction time, and (d) reaction temperature.

of 60 min, and an OA/methanol volume ratio of 1:8. As indicated in Figure 8d, HKUST-1-free exhibited a good catalytic performance at room temperature. A high reaction temperature such as 80 °C is not beneficial, which might be attributed to the evaporation of methanol from the reaction system.

3.4. Reusability of HKUST-1-free. The reusability of HKUST-1-free was evaluated in the esterification of OA with methanol. As shown in Figure 9a, HKUST-1-free can still maintain good catalytic activity with neglected change after 10 cycles. A slight decrease in catalytic activity might be attributed to the adsorption of unreacted OA or methyl oleate on the surface of the catalyst. Although the spent catalyst was washed with ethanol three times after each cycle and dried under vacuum for 12 h at 150 °C for regeneration, a small amount of OA can adsorb onto the surface of the catalyst, perhaps due to the strong coordination of the free carboxylic group in oleic acid with the unsaturated Cu sites. It can be proved by the result from the FT-IR spectroscopy of the spent catalyst (Figure 9b) because the vibration absorption peaks from $-CH_2$ groups on OA/or methyl oleate were observed. Additionally, the structural stability of HKUST-1-free after reuse was testified by XRD. As shown in Figure 9c, the spent catalyst can still maintain the structure of HKUST-1, which is in accordance with the results from nitrogen adsorption that the spent catalyst possesses a lower surface area than the fresh one (Figure 9d).

3.5. Scalable Synthesis of HKUST-1-free. The scalable synthesis of materials is crucial for industrial applications. In this work, a scalable synthesis of HKUST-1-free was attempted. As illustrated in Figure 10, the XRD patterns of HKUST-1-free prepared on a large scale matched well with those on a small scale (Figure 10a). The results from N_2 sorption indicated that HKUST-1-free obtained on a large scale still possessed a high BET surface area of 1187 m^2/g (Figure 10b). Notably, the total mass of HKUST-1-free synthesized by the solvent-free method could reach 14.3 g per 50 mL autoclave with a yield of 92% based on the addition amount of BTC, which is roughly the same as the sample that prepared by the solvothermal method. These results demonstrate that the solvent-free synthesis of HKUST-1-free is scalable.

Currently, the reported solvent-free methods for the synthesis of MOFs mainly involve two modes: ball milling and manual grinding. Both modes can reduce the need for solvents and environmental pollution and improve sustainability.[43,44] Certainly, the mode of ball milling is convenient for practical application. In the laboratory, manual grinding would be adopted due to its facile operation. However, both modes may encounter challenges, such as the difficulty in generating a homogeneous product and controlling the morphology of the product.[45,46] There is no doubt that the solvent-free method is well-consistent with the principles of green chemistry, emphasizing reduced waste and energy consumption.[47−50] While the

https://doi.org/10.1021/acsomega.4c01852
ACS Omega 2024, 9, 37662−37671

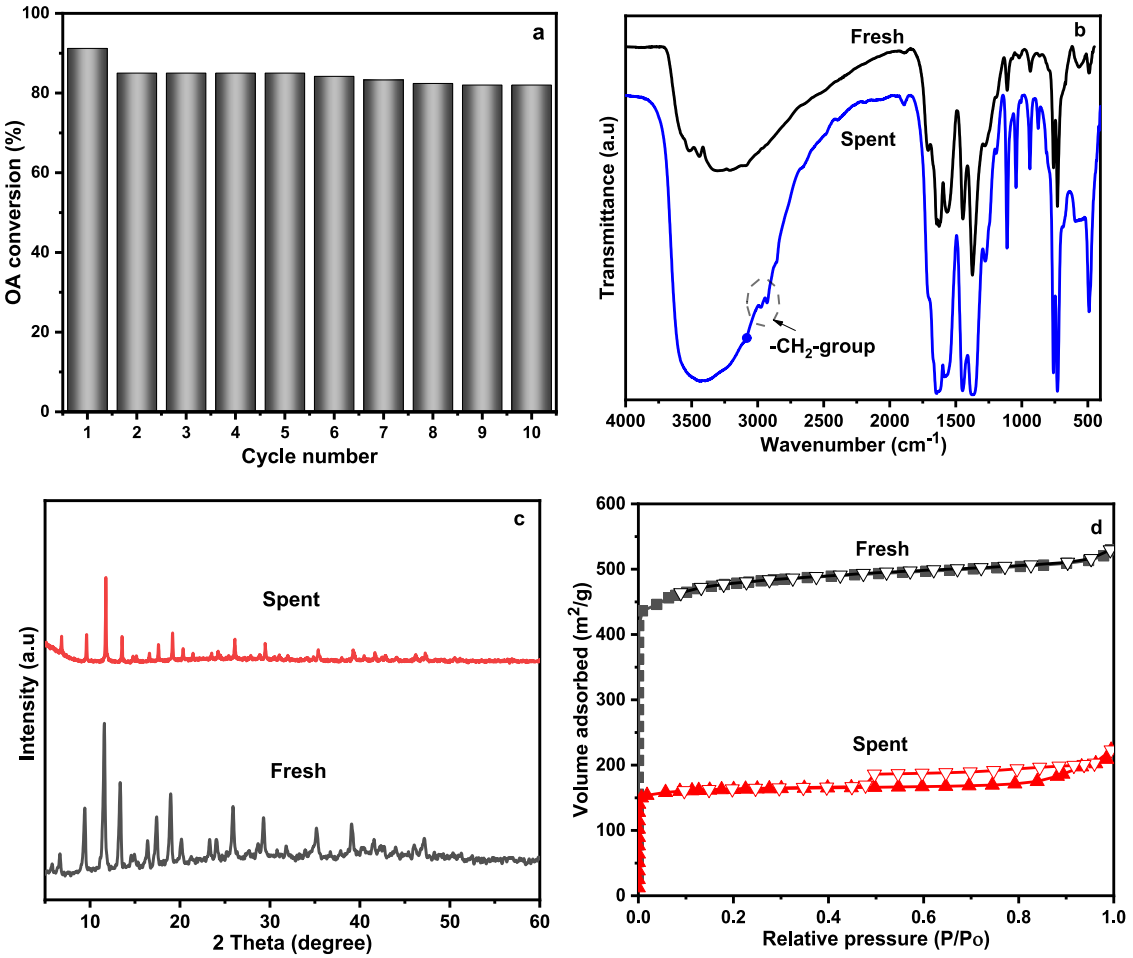

Figure 9. Reusability of HKUST-1-free (a), and FT-IR spectra (b), XRD patterns (c), and N_2 sorption isotherms (d) of fresh and spent HKUST-1-free.

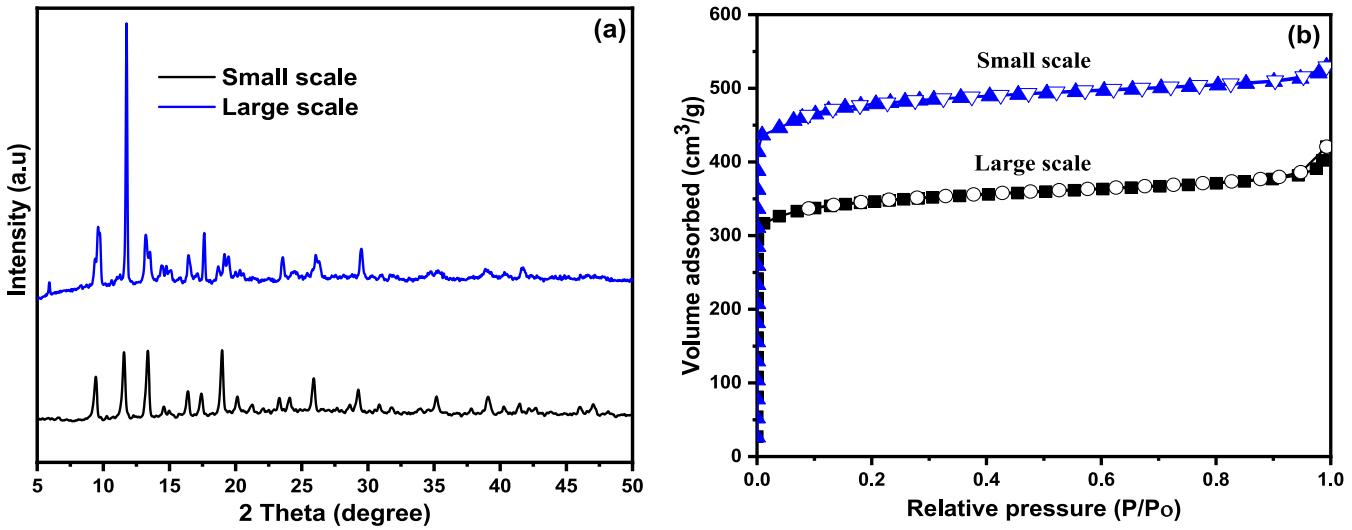

Figure 10. (a) XRD patterns and (b) N_2 sorption isotherms of HKUST-1 prepared on small and large scales.

solvent-free method presents significant environmental and economic benefits, the scalability and the quality of producing MOFs require further optimization.[51,52] Developing the technique could lead to sustainable and industrially viable processes for MOF production, aligned with the broad goals of green chemistry.

4. CONCLUSIONS

In summary, HKUST-1 has successfully been prepared by a solvent-free method. Under the system, the optimization of synthetic parameters has been investigated. The optimized synthetic conditions are a crystallization temperature of 80 °C and a crystallization time of 10 h by using $Cu(NO_3)_2{\cdot}3H_2O$ as

https://doi.org/10.1021/acsomega.4c01852
ACS Omega 2024, 9, 37662−37671

the copper source. The obtained material (HKUST-1-free) possessed a higher surface area and more defect sites than that prepared by the solvothermal method. As a result, HKUST-1-free exhibited superior catalytic activity in the esterification reaction of OA with methanol. The yield of methyl oleate over HKUST-1-free is nearly 1.2 times that over HKUST-1-solvent. Further, the recycling experiment demonstrates that HKUST-1-free is a heterogeneous catalyst and can be reused for several catalytic cycles.

■ ASSOCIATED CONTENT

Supporting Information

The Supporting Information is available free of charge at https://pubs.acs.org/doi/10.1021/acsomega.4c01852.

N_2 adsorption−desorption isotherms of the samples prepared under various synthetic conditions and quantification calculations about the number of defect sites; and XRD patterns of HKUST-1 prepared by using various copper sources (PDF)

■ AUTHOR INFORMATION

Corresponding Authors

Ahmed S. Abou-Elyazed − *MIIT Key Laboratory of Critical Materials Technology for New Energy Conversion and Storage, School of Chemistry and Chemical Engineering, Harbin Institute of Technology, Harbin 150001, China; Chemistry Department, Faculty of Science, Menoufia University, Shebin El-Kom 32512, Egypt;* orcid.org/0000-0003-1607-4496; Email: ahmedphysical90@gmail.com

Yinyong Sun − *MIIT Key Laboratory of Critical Materials Technology for New Energy Conversion and Storage, School of Chemistry and Chemical Engineering, Harbin Institute of Technology, Harbin 150001, China;* orcid.org/0000-0002-5570-5089; Email: yysun@hit.edu.cn

Authors

Abdelhalim I. Ftooh − *Chemistry Department, Faculty of Science, Menoufia University, Shebin El-Kom 32512, Egypt*

Asmaa G. Ashry − *Chemistry Department, Faculty of Science, Menoufia University, Shebin El-Kom 32512, Egypt*

Amira K. F. Shaban − *MIIT Key Laboratory of Critical Materials Technology for New Energy Conversion and Storage, School of Chemistry and Chemical Engineering, Harbin Institute of Technology, Harbin 150001, China*

[‖]**Ahmed M. El-Nahas** − *Chemistry Department, Faculty of Science, Menoufia University, Shebin El-Kom 32512, Egypt;* orcid.org/0000-0002-8547-7574

Ahmed M. Yousif − *Chemistry Department, College of Science, Jouf University, Sakaka 72388, KSA; Chemistry Department, Faculty of Science, Menoufia University, Shebin El-Kom 32512, Egypt*

Complete contact information is available at: https://pubs.acs.org/10.1021/acsomega.4c01852

Notes

The authors declare no competing financial interest.

[‖]Co-author El-Nahas, Ahmed deceased.

■ ACKNOWLEDGMENTS

The authors acknowledge the financial support from the National Natural Science Foundation of China (No. 22172042) and Faculty of Science, Menoufia University.

■ REFERENCES

(1) Zhang, H.; Chen, L.; Li, Y.; Hu, Y.; Li, H.; Xu, C. C.; Yang, S. Functionalized organic-inorganic hybrid porous coordination polymers-based catalysts for biodiesel production via trans/esterification. *Green Chem.* **2022**, *24*, 7763−7786.

(2) Gielen, D.; Boshell, F.; Saygin, D.; Bazilian, M. D.; Wagner, N.; Gorini, R. The role of renewable energy in the global energy transformation. *Energy Strategy Rev.* **2019**, *24*, 38−50.

(3) Tan, H.-T.; Corbin, K. R.; Fincher, G. B. Emerging technologies for the production of renewable liquid transport fuels from biomass sources enriched in plant cell walls. *Front. Plant Sci.* **2016**, *7*, No. 1854.

(4) Zhang, Q.; Wei, F.; Ma, P.; Zhang, Y.; Wei, F.; Chen, H. Mesoporous Al−Mo oxides as an effective and stable catalyst for the synthesis of biodiesel from the esterification of free-fatty acids in non-edible oils. *Waste Biomass Valorization* **2018**, *9*, 911−918.

(5) Ma, X.; Liu, F.; Helian, Y.; Li, C.; Wu, Z.; Li, H.; Chu, H.; Wang, Y.; Wang, Y.; Lu, W. Current application of MOFs based heterogeneous catalysts in catalyzing transesterification/esterification for biodiesel production: A review. *Energy Convers. Manage.* **2021**, *229*, No. 113760.

(6) Cong, W.-J.; Nanda, S.; Li, H.; Fang, Z.; Dalai, A. K.; Kozinski, J. A. Metal−organic framework-based functional catalytic materials for biodiesel production: a review. *Green Chem.* **2021**, *23*, 2595−2618.

(7) Chang, B.; Fu, J.; Tian, Y.; Dong, X. Multifunctionalized ordered mesoporous carbon as an efficient and stable solid acid catalyst for biodiesel preparation. *J. Phys. Chem. C* **2013**, *117*, 6252−6258.

(8) Jha, S. K.; Bilalovic, J.; Jha, A.; Patel, N.; Zhang, H. Renewable energy: Present research and future scope of Artificial Intelligence. *Renewable Sustainable Energy Rev.* **2017**, *77*, 297−317.

(9) Xie, W.; Wan, F. Basic ionic liquid functionalized magnetically responsive Fe3O4@ HKUST-1 composites used for biodiesel production. *Fuel* **2018**, *220*, 248−256.

(10) Lu, T.; Sun, Y.; Shi, M.; Ding, D.; Ma, Z.; Pan, Y.; Yuan, Y.; Liao, W.; Sun, Y. Ni dopped MgAl hydrotalcite catalyzed hydrothermal liquefaction of microalgae for low N, O bio-oil production. *Fuel* **2023**, *333*, No. 126437.

(11) Kuvayskaya, A.; Garcia, S.; Mohseni, R.; Vasiliev, A. Superacidic Mesoporous Catalysts Containing Embedded Heteropolyacids. *Catal. Lett.* **2019**, *149*, 1983−1990.

(12) Kumar, A.; Purwar, P.; Sonkaria, S.; Khare, V. Rationalizing Structural Hierarchy in the Design of Fuel Cell Electrode and Electrolyte Materials Derived from Metal-Organic Frameworks. *Appl. Sci.* **2022**, *12*, 6659.

(13) Suh, M. P.; Park, H. J.; Prasad, T. K.; Lim, D.-W. Hydrogen storage in metal−organic frameworks. *Chem. Rev.* **2012**, *112*, 782−835.

(14) Qiu, S.; Du, J.; Xiao, Y.; Zhao, Q.; He, G. Hierarchical porous HKUST-1 fabricated by microwave-assisted synthesis with CTAB for enhanced adsorptive removal of benzothiophene from fuel. *Sep. Purif. Technol.* **2021**, *271*, No. 118868.

(15) Azad, F. N.; Ghaedi, M.; Dashtian, K.; Hajati, S.; Pezeshkpour, V. Ultrasonically assisted hydrothermal synthesis of activated carbon−HKUST-1-MOF hybrid for efficient simultaneous ultrasound-assisted removal of ternary organic dyes and antibacterial investigation: Taguchi optimization. *Ultrason. Sonochem.* **2016**, *31*, 383−393.

(16) Steenhaut, T.; Grégoire, N.; Barozzino-Consiglio, G.; Filinchuk, Y.; Hermans, S. Mechanochemical defect engineering of HKUST-1 and impact of the resulting defects on carbon dioxide sorption and catalytic cyclopropanation. *RSC Adv.* **2020**, *10*, 19822−19831.

(17) Stolar, T.; Batzdorf, L.; Lukin, S.; Žilić, D.; Motillo, C.; Friščić, T.; Emmerling, F.; Halasz, I.; Užarević, K. In situ monitoring of the mechanosynthesis of the archetypal metal−organic framework HKUST-1: Effect of liquid additives on the milling reactivity. *Inorg. Chem.* **2017**, *56*, 6599−6608.

(18) Pichon, A.; James, S. L. An array-based study of reactivity under solvent-free mechanochemical conditions—insights and trends. *CrystEngComm* **2008**, *10*, 1839−1847.

(19) Liu, P.; Zhao, T.; Cai, K.; Chen, P.; Liu, F.; Tao, D.-J. Rapid mechanochemical construction of HKUST-1 with enhancing water stability by hybrid ligands assembly strategy for efficient adsorption of SF6. *Chem. Eng. J.* **2022**, *437*, No. 135364.

(20) Morales, E. M. C.; Méndez-Rojas, M. A.; Torres-Martínez, L. M.; Garay-Rodríguez, L. F.; López, I.; Uflyand, I. E.; Kharisov, B. I. Ultrafast synthesis of HKUST-1 nanoparticles by solvothermal method: Properties and possible applications. *Polyhedron* **2021**, *210*, No. 115517.
(21) Martínez Gil, J. M.; Reyes, R. V.; Bastidas-Barranco, M.; Giraldo, L.; Moreno-Piraján, J. C. Biodiesel Production from Transesterification with Lipase from Pseudomonas cepacia Immobilized on Modified Structured Metal Organic Materials. *ACS Omega* **2022**, *7*, 41882−41904.
(22) Chowdhury, P.; Bikkina, C.; Meister, D.; Dreisbach, F.; Gumma, S. Comparison of adsorption isotherms on Cu-BTC metal organic frameworks synthesized from different routes. *Microporous Mesoporous Mater.* **2009**, *117*, 406−413.
(23) Park, S. H.; Peralta, R. A.; Moon, D.; Jeong, N. C. Dynamic weak coordination bonding of chlorocarbons enhances the catalytic performance of a metal−organic framework material. *J. Mater. Chem. A* **2022**, *10*, 23499−23508.
(24) Abou-Elyazed, A. S.; Ye, G.; Sun, Y.; El-Nahas, A. M. A series of UiO-66 (Zr)-structured materials with defects as heterogeneous catalysts for biodiesel production. *Ind. Eng. Chem. Res.* **2019**, *58*, 21961−21971.
(25) Abou-Elyazed, A. S.; Sun, Y.; El-Nahas, A. M.; Yousif, A. M. A green approach for enhancing the hydrophobicity of UiO-66 (Zr) catalysts for biodiesel production at 298 K. *RSC Adv.* **2020**, *10*, 41283−41295.
(26) Klimakow, M.; Klobes, P.; Rademann, K.; Emmerling, F. Characterization of mechanochemically synthesized MOFs. *Microporous Mesoporous Mater.* **2012**, *154*, 113−118.
(27) Duan, C.; Yu, Y.; Li, F.; Wu, Y.; Xi, H. Ultrafast room-temperature synthesis of hierarchically porous metal−organic frameworks with high space−time yields. *CrystEngComm* **2020**, *22*, 2675−2680.
(28) Heo, C. Y.; Díaz-Ramírez, M. L.; Park, S. H.; Kang, M.; Hong, C. S.; Jeong, N. C. Solvent-Driven Dynamics: Crafting Tailored Transformations of Cu (II)-Based MOFs. *ACS Appl. Mater. Interfaces* **2024**, *16* (7), 9068−9077.
(29) Hu, Z.; Castano, I.; Wang, S.; Wang, Y.; Peng, Y.; Qian, Y.; Chi, C.; Wang, X.; Zhao, D. Modulator effects on the water-based synthesis of Zr/Hf metal−organic frameworks: Quantitative relationship studies between modulator, synthetic condition, and performance. *Cryst. Growth Des.* **2016**, *16*, 2295−2301.
(30) Szufla, M.; Navarro, J. A.; Góra-Marek, K.; Matoga, D. Effect of Missing-Linker Defects and Ion Exchange on Stability and Proton Conduction of a Sulfonated Layered Zr-MOF. *ACS Appl. Mater. Interfaces* **2023**, *15*, 28184−28192.
(31) Singha, S.; Saha, A.; Goswami, S.; Dey, S. K.; Payra, S.; Banerjee, S.; Kumar, S.; Saha, R. A Metal−Organic Framework to CuO Nanospheres of Uniform Morphology for the Synthesis of α-Aminonitriles under Solvent-Free Condition along with Crystal Structure of the Framework. *Cryst. Growth Des.* **2018**, *18*, 189−199.
(32) Dubale, A. A.; Su, W.-N.; Tamirat, A. G.; Pan, C.-J.; Aragaw, B. A.; Chen, H.-M.; Chen, C.-H.; Hwang, B.-J. The synergetic effect of graphene on Cu 2 O nanowire arrays as a highly efficient hydrogen evolution photocathode in water splitting. *J. Mater. Chem. A* **2014**, *2*, 18383−18397.
(33) Dubale, A. A.; Ahmed, I. N.; Chen, X.-H.; Ding, C.; Hou, G.-H.; Guan, R.-F.; Meng, X.; Yang, X.-L.; Xie, M.-H. A highly stable metal−organic framework derived phosphorus doped carbon/Cu 2 O structure for efficient photocatalytic phenol degradation and hydrogen production. *J. Mater. Chem. A* **2019**, *7*, 6062−6079.
(34) Zhang, Q.; Luo, Q.; Wu, Y.; Yu, R.; Cheng, J.; Zhang, Y. Construction of a Keggin heteropolyacid/Ni-MOF catalyst for esterification of fatty acids. *RSC Adv.* **2021**, *11*, 33416−33424.
(35) Abou-Elyazed, A.; Sun, Y.; El-Nahas, A.; Abdel-Azeim, S.; Sharara, T.; Yousif, A. Solvent-free synthesis and characterization of Ca^{2+}-doped UiO-66 (Zr) as heterogeneous catalyst for esterification of oleic acid with methanol: a joint experimental and computational study. *Mater. Today Sustainability* **2022**, *18*, No. 100110.
(36) Zhou, K.; Chaemchuen, S. Metal-organic framework as catalyst in esterification of oleic acid for biodiesel production. *Int. J. Environ. Sci. Dev.* **2017**, *8*, 251.
(37) Zhang, Q.; Liu, X.; Yang, T.; Yue, C.; Pu, Q.; Zhang, Y. Facile synthesis of polyoxometalates tethered to post Fe-BTC frameworks for esterification of free fatty acids to biodiesel. *RSC Adv.* **2019**, *9*, 8113−8120.
(38) Abou-Elyazed, A. S.; Shaban, E. A.; Sun, Y.; El-Nahas, A. M.; Kashar, T. I. Solvent-Free Synthesis and Characterization of Bimetallic UiO-66 (Zr/Sn) Heterogeneous Catalyst for Biodiesel Production. *Ind. Eng. Chem. Res.* **2023**, *62*, 9211−9220.
(39) Gouda, S. P.; Dhakshinamoorthy, A.; Rokhum, S. L. Metal-organic framework as a heterogeneous catalyst for biodiesel production: A review. *Chem. Eng. J. Adv.* **2022**, *12*, No. 100415.
(40) Hommes, A.; Heeres, H. J.; Yue, J. Catalytic transformation of biomass derivatives to value-added chemicals and fuels in continuous flow microreactors. *ChemCatChem* **2019**, *11*, 4671−4708.
(41) Brahma, S.; Nath, B.; Basumatary, B.; Das, B.; Saikia, P.; Patir, K.; Basumatary, S. Biodiesel production from mixed oils: A sustainable approach towards industrial biofuel production. *Chem. Eng. J. Adv.* **2022**, *10*, No. 100284.
(42) Abou-Elyazed, A. S.; Shaban, A. K.; Osman, A. I.; Heikal, L. A.; Mohamed, H. F.; Hassan, W. M.; El-Nahas, A. M.; Keshta, B. E.; Hamouda, A. S. Comparative catalytic efficacy of cost-effective MIL-101 (Cr) based PET waste for biodiesel production, Current Research in Green and Sustainable. *Chemistry* **2024**, *8*, No. 100401.
(43) James, S. L.; Adams, C. J.; Bolm, C.; Braga, D.; Collier, P.; Friščić, T.; Waddell, D. C. Mechanochemistry: opportunities for new and cleaner synthesis. *Chem. Soc. Rev.* **2012**, *41*, 413−447.
(44) Friščić, T.; Mottillo, C.; Titi, H. M. Mechanochemistry for synthesis. *Angew. Chem.* **2020**, *132*, 1030−1041.
(45) Chen, B.; Xiang, S.; Qian, G. Metal− organic frameworks with functional pores for recognition of small molecules. *Acc. Chem. Res.* **2010**, *43*, 1115−1124.
(46) Karami, A.; Mohamed, O.; Ahmed, A.; Husseini, G. A.; Sabouni, R. Recent advances in metal-organic frameworks as anticancer drug delivery systems: A review. *Anticancer Agents Med. Chem.* **2021**, *21*, 2487−2504.
(47) Férey, G. Hybrid porous solids: past, present, future. *Chem. Soc. Rev.* **2008**, *37*, 191−214.
(48) Szczęśniak, B.; Borysiuk, S.; Choma, J.; Jaroniec, M. Mechanochemical synthesis of highly porous materials. *Mater. Horiz.* **2020**, *7*, 1457−1473.
(49) Sun, D. W.; Huang, L.; Pu, H.; Ma, J. Introducing reticular chemistry into agrochemistry. *Chem. Soc. Rev.* **2021**, *50*, 1070−1110.
(50) Głowniak, S.; Szczęśniak, B.; Choma, J.; Jaroniec, M. Mechanochemistry: Toward green synthesis of metal−organic frameworks. *Mater. Today* **2021**, *46*, 109−124.
(51) Ye, G.; Zhang, D.; Li, X.; Leng, K.; Zhang, W.; Ma, J.; Ma, S. Boosting catalytic performance of metal−organic framework by increasing the defects via a facile and green approach. *ACS Appl. Mater. Interfaces* **2017**, *9*, 34937−34943.
(52) Ariga, K. Materials nanoarchitectonics at dynamic interfaces: Structure formation and functional manipulation. *Materials* **2024**, *17*, 271.

https://doi.org/10.1021/acsomega.4c01852
ACS Omega 2024, 9, 37662−37671